Journal of Molecular Structure 1005 (2011) 17–24

Contents lists available at SciVerse ScienceDirect

Journal of Molecular Structure

journal homepage: www.elsevier.com/locate/molstruc

Infrared and Raman spectroscopic analysis and theoretical computation of the first hyperpolarizability of a monoarylated anthraquinone, 1-(4-methoxyphenyl)-4-methylanthraquinone

Tomy Joseph [a], Hema Tresa Varghese [b], C. Yohannan Panicker [c,d,*], Thies Thiemann [e,1], K. Viswanathan [f], Christian Van Alsenoy [g]

[a] Department of Physics, St. Xavier's College, Vaikom, Kothavara, Kottayam, Kerala, India
[b] Department of Physics, Fatima Mata National College, Kollam, Kerala, India
[c] Department of Physics, TKM College of Arts and Science, Kollam, Kerala, India
[d] Research Centre, Department of Physics, Mar Ivanios College, Nalanchira, Trivandrum, Kerala, India
[e] Graduate School of Interdisciplinary Engineering Sciences, Kyushu University, Fukuoka, Japan
[f] Department of Physics, Karpagam University, Pollachi Main Road, Eachanari, Coimbatore, Tamilnadu, India
[g] University of Antwerp, Chemistry Department, Universiteitsplein 1, B2610 Antwerp, Belgium

ARTICLE INFO

Article history:
Received 28 June 2011
Received in revised form 28 July 2011
Accepted 28 July 2011
Available online 19 August 2011

Keywords:
Anthraquinone
Infrared spectroscopy
Raman spectroscopy
Hyperpolarizability
DFT calculation

ABSTRACT

Infrared and Raman spectroscopic analyses were carried out on 1-(4-methoxyphenyl)-4-methylanthraquinone (**1**). The interpretation of the spectra was aided by DFT calculations of the molecule. The vibrational wavenumbers were examined theoretically using the Gaussian 03 set of quantum chemistry codes, and the normal modes were assigned by potential energy distribution (PED) calculations. A computation of the first hyperpolarizability of the compound indicates that this class of substituted anthraquinones may be a good candidate as a NLO material. Optimized geometrical parameters of the compound are in agreement with similar reported structures.

1. Introduction

Arylated anthraquinones such as **1** (Fig. 1) have generated interest in physical organic chemistry [1,2] due to the interaction of the attached aryl groups with the π-system of the anthraquinone core as evidenced in the UV and luminescence [3,4] spectra, and in the redox behavior of the molecules [2,5]. Specifically, the interaction of the substituents on the C=O function of the anthraquinones has been investigated [1]. In practical applications, arylated anthraquinones have been used as stabilizers of light-modulating fluids such as of liquid polybenzyltoluenes [6]. Matsuura et al. [7] reported the absorption maxima of various organic dyes such as indigo, azobenzene, phenylamine, hydrazone, anthraquinone, naphthoquinone, and malachite green using the AM1, PM3 and PM5 semiempirical molecular orbital theories with the configuration interaction singles and random phase approximation approaches. Sasirekha and Ramakrishnan [8] reported the role of solute–solvent and solvent–solvent interaction of the preferential salvation characteristics of 2,6-diaminoanthraquinone by monitoring the optical absorption and fluorescence emission spectra. Light scattering determination of viscoelastic and electro-optic parameters of azo and anthraquinone dye-doped liquid crystal molecules and consistent neural network empirical physical formula construction for scattering intensities was reported by Yildiz et al. [9]. Spectroscopic characterization of effective components of anthraquinones in Chinese medicinal herbs binding with serum albumins was reported by Bi et al. [10]. The UV/Vis absorption spectra of 101 anthraquinones solvated in methanol and ethanol have been theoretically predicted by Jacquemin et al. [11] using the time dependent density functional theory for the excited state calculations and the polarizable continuum model for evaluating bulk solvent effects. Synthesis, optical and electrochemical properties of new receptors and sensors containing anthraquinone and benzimidazole units were reported by Wannalerse et al. [12]. Of late, however, push–pull anthraquinones [13] and anthraquinones as acceptors linked to various electron donors such as ferrocene [14] have also been found to have interesting nonlinear optical properties. In general, nonlinear optics (NLO) deals with

* Corresponding author at: Department of Physics, TKM College of Arts and Science, Kollam, Kerala, India. Tel.: +91 9895370968.
E-mail address: cyphyp@rediffmail.com (C.Y. Panicker).
[1] Present address: United Arab Emirates University, Al Ain, United Arab Emirates.

0022-2860/$ - see front matter © 2011 Elsevier B.V. All rights reserved.
doi:10.1016/j.molstruc.2011.07.060

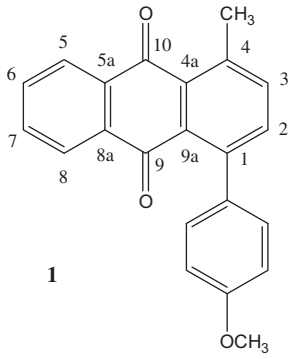

1

Fig. 1. 1-(4-Methoxyphenyl)-4-methylanthraquinone.

the interaction of materials with applied electromagnetic fields to generate new electromagnetic fields, altered in wavenumber, phase, or other physical properties [15], where organic molecules able to manipulate photonic signal efficiently in this way are of importance in technologies such as optical communication, optical computing, and dynamic image processing [16,17]. In this context, surprisingly phenyl substituents can increase the hyperpolarizability of molecules [18,19], a result described as surprising. Recently, the authors have reported on a novel synthesis of arylated anthraquinones [20], with the cycloaddition of substituted of halogenated thiophene *S*-oxides to benzoquinones and subsequent Suzuki cross-coupling reactions as key steps of the synthesis. In the present communication, the infrared and Raman spectroscopic analysis of 1-(4-methoxyphenyl)-4-methylanthraquinone (Fig. 1) as one new representative of a series of arylated anthraquinones available through this synthesis are reported. Additionally, a theoretical computation of the first hyperpolarizability of the compound is presented.

2. Experimental

2.1. Synthesis (Fig. 2)

In an inert atmosphere, a solution of 1-bromo-4-methylanthraquinone (267 mg, 0.89 mmol), 4-methoxyphenylboronic acid (430 mg, 2.83 mmol), $Pd(PPh_3)_2Cl_2$ (30 mg, 4.0×10^{-5} mol) and triphenylphosphine (30 mg, 0.11 mmol) in a solvent mixture of DME (10 mL) and aq. Na_2CO_3 (2.32 g Na_2CO_3 in 15 ml H_2O, 6 mL) was kept at 65 °C for 18 h. Thereafter, the cooled solution was poured into water (25 mL) and extracted with chloroform (3×15 mL). The combined organic phase was dried over anhydrous $MgSO_4$ and was concentrated *in vacuo*. Column chromatography of the residue on silica gel (hexane/$CHCl_3$/ether 3:1:1) gave 1-(4-methoxyphenyl)-4-methyl-anthraquinone (**1**) (210 mg, 72%). – yellow–orange needles; mp. 221 °C; δ_H (270 MHz, $CDCl_3$) 2.88 (3H, s, CH_3), 3.88 (3H, s, OCH_3), 6.97 (2H, d, ^3J = 8.6 Hz), 7.20 (2H, d, ^3J = 8.6 Hz), 7.44 (1H, d, ^3J = 8.1 Hz), 7.53 (1H, d, ^3J = 8.1 Hz), 7.67–7.75 (2H, m), 8.04–8.07 (1H, m), 8.19–8.23 (1H, m); δ_C (67.8 MHz, $CDCl_3$) 23.8 (CH_3), 55.2 (OCH_3), 113.6 (2C, CH), 126.6 (CH), 129.2 (2C, CH), 132.8 (C_{quat}), 132.9 (Cquat), 133.5 (CH), 133.6 (CH), 134.1 (Cquat), 134.2 (Cquat), 134.8 (Cquat), 137.0 (CH, 3C), 141.3 (Cquat), 142.6 (Cquat), 158.7 (Cquat), 184.6 (Cquat, CO), 184.7 (Cquat, CO); MS (FAB, 3-nitrobenzyl alcohol) *m*/*z* (%) 329 (MH^+) (14). HRMS Found: 329.1183. Calcd. for $C_{22}H_{17}O_3$: 329.1178 (MH^+, FAB). Found: C, 80.30; H, 4.76%. Calcd. for $C_{22}H_{16}O_3$: C, 80.47; H, 4.91%; UV–Vis spectrum (CH_3CN, nm) λ_{max} 253 (38,343), 269 (sh, 15,440), 302 (5400), 354 (2505).

2.2. IR and Raman spectroscopy

The FT-IR spectrum (Fig. 3) was recorded using a Perkin Elmer FT-IR Spectrometer Spectrum RX1 with KBr pellets, number of scans 16, resolution 2 cm^{-1}. The FT-Raman spectrum (Fig. 4) was obtained on a Bruker Equinox 55/s spectrometer with the FRA emission of a Nd:YAG laser with an excitation wavelength of λ = 1064 nm, a laser power of 250 mW, and a resolution of 2 cm^{-1} (number of scans: 128). The measurement was carried out on the solid sample.

3. Computational details

For meeting both the requirements of accuracy and computing economy, theoretical methods and basis sets should be considered. DFT has proven to be extremely useful in treating electronic structures of molecules of similar complexity as **1**. The basis set 6-31G(d,p) has been used previously as an effective and economical tool to study these fairly large organic molecules. Based on these points, the density functional three-parameter hybrid model (DFT/B3LYP) at the 6-31G(d,p) basis set level along with the HF method was adopted to calculate the properties of the studied molecule in this work. All the calculations were performed using the Gaussian 03W program package [21] with the default convergence criteria without any constraint on the geometry [22]. Scaling factors 0.9613 and 0.8929 has been uniformly applied for the DFT and HF calculated frequencies [23]. The potential energy distribution (PED) was calculated with the help of the GAR2PED software package [24]. The obtained (DFT) geometrical parameters (Fig. 5) are given as Supplementary material (Table S1). Potential energy surface scan studies have been carried out to understand the stability of planar and non-planar structures of the molecule. The profiles of potential energy surface for torsion angles C_{32}—O_{31}—C_{28}—C_{26} and C_{26}—C_{23}—C_{21}—C_5 are given in Figs. 6 and 7. The energy is minimum for −1.1° (−1073.65432 Hartree) and 175.6° (−1073.65296 Hartree) for the above torsion angles.

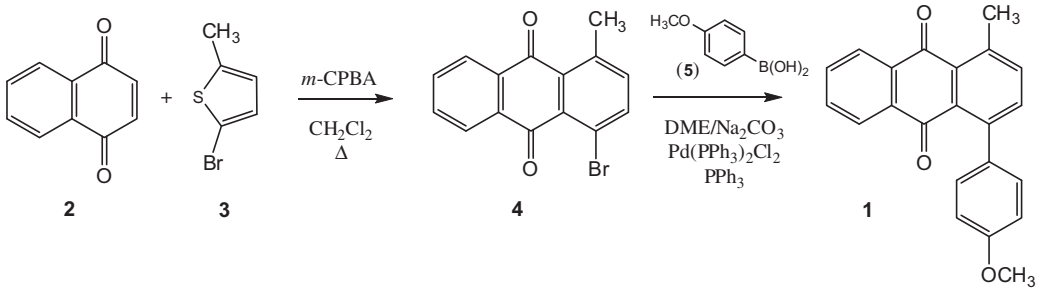

2 3 4 1

Fig. 2. Synthesis of 1-(4-methoxyphenyl)-4-methylanthraquinone (**1**).

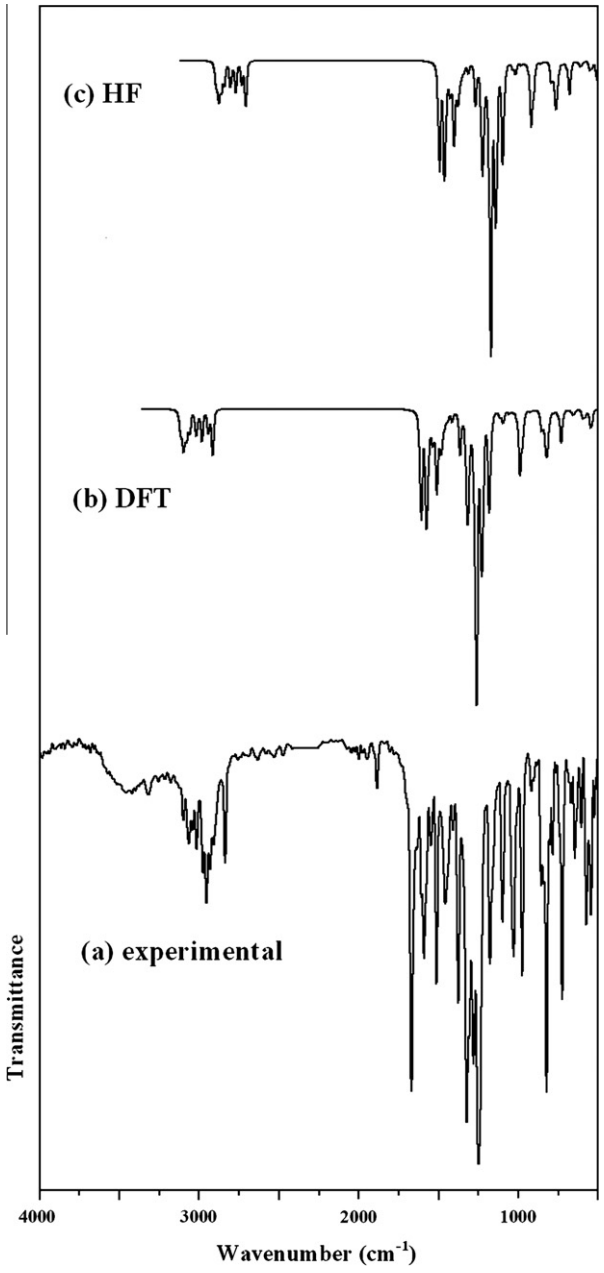

Fig. 3. FT-IR spectrum: (a) experimental, (b) DFT and (c) HF.

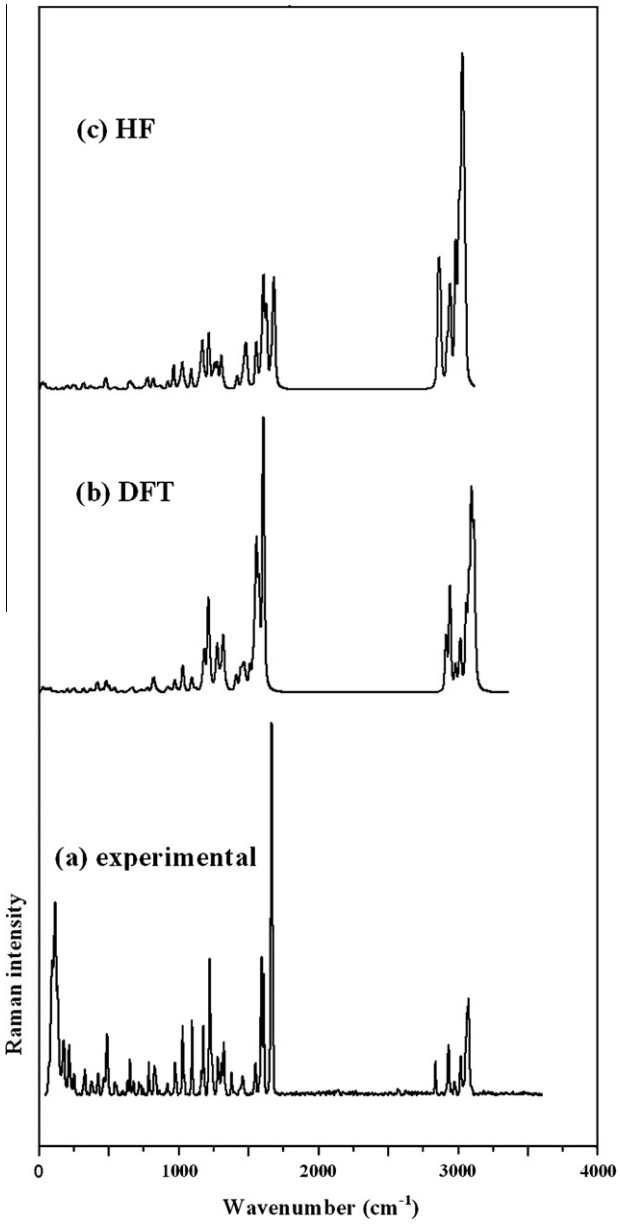

Fig. 4. FT-Raman spectrum: (a) experimental, (b) DFT and (c) HF.

4. Results and discussion

4.1. IR and Raman spectra

The observed IR and Raman bands with their relative intensities and calculated (scaled) wavenumbers and assignments are given in Table 1.

Infrared active C═O stretching vibrations for anthraquinones have been reported in the region 1680–1630 cm^{-1}, with anthraquinone itself at 1676 cm^{-1} [25], 2-methylanthraquinone at 1672 cm^{-1} [19], 1,4-dimethylanthraquinone at 1668 cm^{-1} [19], and 2-hydroxymethylanthraquinone at 1679 cm^{-1} [25]. While few Raman spectra of anthraquinones have been published, Jorge-Villar and Edwards [26] reported the characteristic Raman bands of the anthraquinone pigment, atranorin. Baran et al. [27] published the Raman spectrum of the 1,2-dihydroxyanthraquinone, alizarin, adsorbed on a silver surface with υC═O at 1657 and at 1629 cm^{-1},

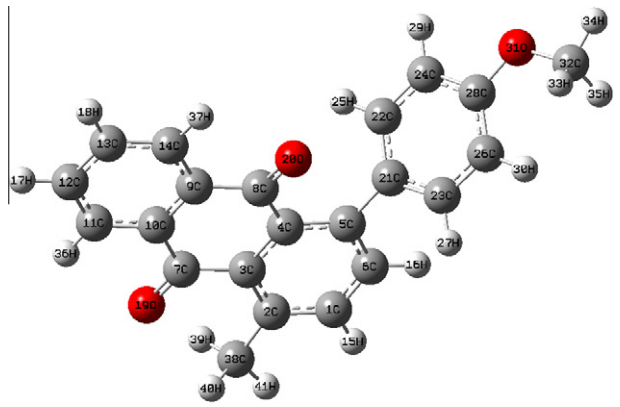

Fig. 5. Optimized geometry (DFT) of the molecule.

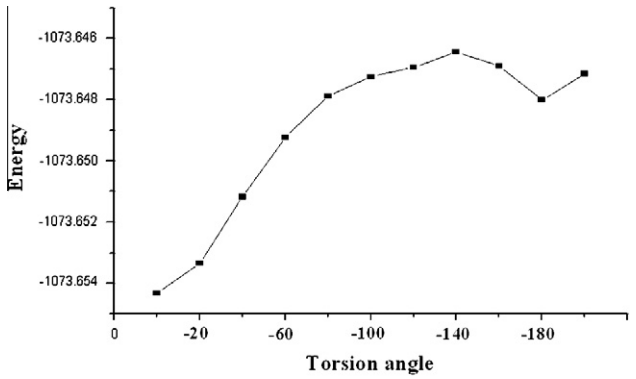

Fig. 6. Profile of potential energy scan for the torsion angle C_{32}—O_{31}—C_{28}—C_{26}.

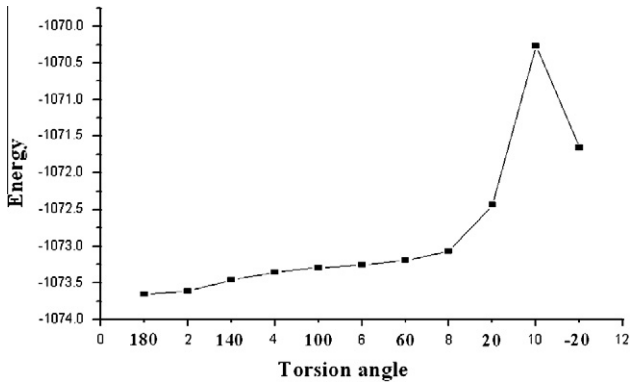

Fig. 7. Profile of potential energy scan for the torsion angle C_{26}—C_{23}—C_{21}—C_5.

where it is known that the intramolecular hydrogen bonding from the hydroxyl group to the quinone carbonyl function decreases the band frequency versus a non-complexed carbonyl function. Krishnakumar and Xavier [28] reported the Raman spectrum of 1,5-dichloroanthraquinone. While no frequency was assigned to a C═O stretching vibration for 1,5-dichloroanthraquinone, it is most likely the reported, but differently assigned signal at 1663 cm^{-1}, with the IR active υC═O at 1697 cm^{-1} rather than associated with the assigned bands at 1823 cm^{-1} and 1792 cm^{-1} [28]. These results would be in-line with the spectrum of our title compound **1**, for which the C═O stretching vibrations were observed at 1669, 1600 cm^{-1} in the IR spectrum, at 1664, 1609 cm^{-1} in the Raman spectrum and were found to be at 1610, 1606 cm^{-1} theoretically, according to B3LYP calculations. The in-plane δC═O and out-of-plane γC═O deformation bands were also identified and assigned (Table 1).

In the present discussion, the methyl (CH_3) group attached to the anthraquinone core at C_2 and the methoxy group attached to the phenyl substituent at C_5 of the anthraquinone are designated as, MeI and MeII. The stretching vibrations of the CH_3 group are expected in the range of 2900–3050 cm^{-1} [29,30]. The asymmetric stretching modes of the methyl group are calculated to be at 3057, 2982 cm^{-1} for MeII and at 3017, 3013 cm^{-1} for MeI and the symmetric modes at 2914 (MeII) and at 2941 cm^{-1} (MeI). The bands observed at 3051, 3016, 2976 cm^{-1} in the infrared spectrum and at 3018, 2977 cm^{-1} in the Raman spectrum were assigned as asymmetric stretching modes of the CH_3 group. The symmetric stretching modes were observed at 2954, 2932 cm^{-1} in the IR spectrum and at 2931 cm^{-1} in the Raman spectrum. The asymmetric and symmetric bending vibrations of the methyl group normally appear in the region of 1400–1485 cm^{-1} and 1380–1420 cm^{-1} [30,31]. The bands observed at 1458, 1383 cm^{-1} in the IR spectrum and at 1438, 1380 cm^{-1} in the Raman spectrum was assigned as CH_3 bending modes. The B3LYP calculations give these modes in the range of 1409–1485 cm^{-1}.

Aromatic molecules display a methyl rocking mode in the neighborhood of 1045 cm^{-1} and the second rocking band in the region of 970 ± 70 cm^{-1} [30]. In the present case the rocking modes of MeI were calculated to be at 1055, 1038 and 972 cm^{-1} and were observed at 1034, 968 cm^{-1} experimentally. For the methyl group, MeII, these modes were assigned to signals at 1159, 1121 cm^{-1} theoretically, where only one band was observed in the Raman spectrum at 1159 cm^{-1}. The torsional vibrations of methyl groups often were assigned within the region 185 ± 65 cm^{-1} [30].

In the following discussion, the benzoannelation of the quinone system Qring are designated as PhI, and PhIII, respectively, with PhI-Qring-PhIII representing the anthraquinone core. The para substituted phenyl ring is designated as PhII. The modes in the benzo rings and the phenyl substituent will differ in wavenumber, and the magnitude of splitting will depend on the strength of interaction between different parts (internal coordinates) of the rings. For some modes, this splitting is so small that they may be considered as quasi-degenerate and for other modes a significant amount of splitting is observed [32–35]. The CH stretching vibrations of the phenyl ring are expected in the region 3000–3120 cm^{-1} [30]. The calculated (DFT) values for these modes lie in the region of 3075–3118 cm^{-1}. The bands observed at 3113, 3083, 3070 cm^{-1} in the IR spectrum and at 3075 cm^{-1} in the Raman spectrum are assigned as υCH modes of the phenyl ring.

The benzene ring possesses six ring stretching vibrations, of which the four with the highest wavenumbers (occurring respectively near 1600, 1580, 1490 and 1440 cm^{-1}) are good group vibrations [30]. The fifth ring stretching vibration is active near 1315 ± 65 cm^{-1}, a region which overlaps strongly with that of the CH in-plane deformation. The sixth ring stretching vibration or ring breathing mode appears as a weak band near 1000 cm^{-1} in mono, 1,3-di- and 1,3,5-tri-substituted benzenes. In the otherwise substituted benzenes, however, this vibration is substituent sensitive [30]. The bands observed in the range 1029–1590 cm^{-1} in the IR spectrum, 1029–1594 cm^{-1} in the Raman spectrum and 1009–1610 cm^{-1} (DFT) are assigned as υPh modes. Some phenyl ring stretching modes υPh are not pure, but contain significant contributions from other modes, also.

For the phenyl ring υPhI, the ring breathing mode was assigned theoretically at 1094 cm^{-1} and was observed experimentally at 1100 cm^{-1} in the IR spectrum and at 1096 cm^{-1} in the Raman spectrum. The ring breathing mode for para-disubstituted benzenes with entirely different substituents are expected to be strongly IR active with typical bands in the interval of 780–840 cm^{-1} [36]. For the title compound, this band was confirmed by the strong band in the IR spectrum at 778 cm^{-1} which finds support from computational results. Ambujakshan et al. [37] reported a value 792 cm^{-1} (IR) and 782 cm^{-1} (calculated) as ring breathing mode of para substituted benzenes. In overall comparison, Baran et al. [27] reported υQring 1273, 1143, 1090, 1044, 1027 cm^{-1}, δQring 1292, 823 cm^{-1} in the Raman spectrum of the silver surface complexed anthraquinone alizarin.

According to Roeges [30], in the case of ortho-substitution only one strong absorption in the region 755 ± 35 cm^{-1} is observed and is due to the out-of-plane γCH mode. This was confirmed by the presence of a strong band at 733 cm^{-1} in the IR spectrum and was supported by the calculated result at 730 cm^{-1}. Two very strong γCH deformation bands, occurring at 840 ± 50 cm^{-1}, are typical for 1,4-di-substituted benzenes [30]. For the title compound, a very strong γCH was observed at 824 cm^{-1} in the IR spectrum. Again according to the literature [29,35] a low γCH absorption can be found in the neighborhood, at 820 ± 45 cm^{-1}, but it is much weaker or infrared inactive. The DFT calculations

Table 1
Calculated vibrational wavenumbers (scaled), measured infrared and Raman bands positions and assignments.

HF/6-31G*			B3LYP/6-31G*			IR υ (cm^{-1})	Raman υ (cm^{-1})	Assignments
υ (cm^{-1})	IR intensity	Raman activity	υ (cm^{-1})	IR intensity	Raman activity			
3049	9.86	156.40	3118	16.40	207.54	3113 w		υCH I (100)
3046	1.33	24.60	3114	1.25	28.98			υCH I (94)
3039	5.95	155.70	3111	7.02	194.52			υCH II (96)
3035	17.03	94.55	3109	17.30	57.41			υCH II (92)
3025	18.57	168.25	3096	17.21	183.70			υCH III (98)
3024	23.31	166.30	3095	23.58	193.41			υCH I (99)
3007	4.94	72.91	3083	13.39	36.57	3083 w		υCH II (99)
3006	8.45	73.81	3079	4.71	80.11			υCH I (94)
3004	20.61	39.77	3076	3.51	43.52			υCH II (50), υCH III (45)
3003	12.08	54.37	3075	22.38	100.61	3070 w	3075 s	υCH II (41), υCH III (55)
2981	35.44	161.74	3057	26.06	168.95	3051 w		υ_{as}Me II (90)
2947	9.27	72.29	3017	28.20	76.39	3016 m	3018 m	υ_{as}Me I (94)
2937	25.02	75.47	3013	9.98	75.96			υ_{as}Me I (100)
2922	48.50	48.33	2982	42.99	61.56	2976 m	2977 w	υ_{as}Me II (100)
2871	34.88	161.71	2941	27.26	241.07	2954 m	2931 m	υ_{s}Me I (100)
2859	47.36	120.36	2914	60.93	135.69	2932 m		υ_{s}Me II (100)
1683	68.84	186.28	1610	64.64	60.41	1669 vs	1664 vs	$\upsilon C_8{=}O_{20}$ (53), υPh I (37)
1666	328.92	43.92	1606	73.68	434.50	1600 sh	1609 s	$\upsilon C_7{=}O_{19}$ (52), υPh II (39)
1629	58.13	123.31	1605	23.63	181.37	1590 s	1594 s	υPh II (60)
1608	72.54	109.04	1574	152.48	124.04	1578 w		$\upsilon C_7{=}O_{19}$ (21), $\upsilon C_8{=}O_{20}$ (18), υPh I (60)
1597	2.60	38.02	1573	2.61	151.44			υPh I (40), υPh III (35)
1591	3.25	8.92	1565	28.12	3.75			υPh II (63)
1584	15.66	12.89	1554	16.63	406.44		1551 m	$\upsilon C_7{=}O_{19}$ (31), $\upsilon C_8{=}O_{20}$ (15), υPh I (26), υPh III (27)
1556	35.92	67.26	1534	51.17	75.12			υPh III (66), δCH III (16)
1521	148.34	2.02	1509	99.04	51.44	1512 s	1511 w	υPh II (46), δCH II (48)
1491	1.65	0.86	1485	63.63	13.36			δ_{as}Me II (92)
1490	38.08	16.99	1479	2.97	1.53			υPh I (45), δCH I (52)
1483	8.30	33.48	1473	8.77	38.41			δ_{as}Me II (97)
1474	8.70	13.36	1465	9.09	14.60			δ_{as}Me I (77)
1469	6.55	25.61	1461	6.97	27.59	1458 m		δ_{as}Me I (91)
1467	15.04	3.50	1454	4.94	14.21		1455 w	υPh I (62), δCH I (30)
1457	1.26	2.86	1445	0.36	40.27			υPh III (45), δCH III (15), δCH I (12)
1453	15.78	8.74	1440	10.58	12.71		1438 w	δ_{s}Me II (78)
1421	6.54	13.88	1413	11.32	17.70			δ_{s}Me I (70)
1410	2.40	3.80	1409	1.93	30.64	1383 w	1380 m	δ_{s}Me I (27), υPh II (44), δCH II (27)
1378	54.43	0.63	1364	56.27	1.64	1377 s		υQRing (55), δCH III (22)
1323	1.88	4.06	1341	3.21	10.88			υPh I (86)
1307	65.19	37.57	1321	77.84	85.65	1324 vs	1323 m	υPh III (58), δCH II (41)
1302	250.21	15.55	1318	78.11	73.97			υPh II (47), δCH II (37)
1277	78.42	26.86	1305	38.46	6.83			υPh II (63)
1260	334.79	21.26	1300	2.62	35.99	1294 w	1296 m	υQRing (60), δCH I (22)
1254	17.14	7.89	1275	54.00	142.49	1282 vs	1280 m	$\upsilon C_5{-}C_{21}$ (33), δCH III (40)
1245	5.71	14.78	1262	416.53	14.79	1250 vs		υPh III (46), υQRing (33)
1217	99.33	82.49	1242	8.06	5.27		1235 w	υPh I (26), δCH I (44), δCCCQ (20)
1192	23.38	5.46	1227	271.21	17.78		1223 s	$\upsilon C_{28}{-}O_{31}$ (50), υPh II (27), δCH II (13)
1186	30.25	3.10	1214	0.85	265.31			$\upsilon C_2{-}C_{38}$(35), υPh III (45)
1182	41.28	8.06	1188	0.64	35.89			υPh III (39), δCH III (59)
1171	42.52	46.13	1182	112.03	64.76	1178 s		δCH III (63)
1164	14.36	9.50	1173	16.41	11.32		1175 s	δCH I (80)
1161	8.18	10.36	1168	13.14	4.17			δCCC III (29), δCCC I (23), δCCC Q (29),
1154	0.98	15.04	1159	0.34	8.15		1159 w	δMe II (76)
1139	2.07	7.05	1121	0.31	8.46			δMe II (97)
1105	9.53	0.62	1113	7.95	1.80			υPh II (32), δCH II (61)
1095	0.49	1.26	1094	0.72	2.40	1100 s	1096 s	υPh I (27), δCH I (29), δCCC I (43)
1090	32.25	22.35	1093	19.25	43.21			δCH III (30), υQRing (33), υPh III (35)
1085	3.90	0.51	1055	5.78	0.57			δMe I (68), γCC_{38} (10)
1072	0.03	0.63	1038	1.47	5.95		1034 w	δMe I (31), υPh I (27), υPh II (29)
1042	7.18	6.86	1029	1.34	61.21	1029 s	1029 s	υPh I (47), δMe I (19), δCH I (13)
1039	4.59	2.56	1009	0.07	0.24			γCH I (84)
1036	0.87	1.60	1009	6.26	1.24			δCCC II (51), υPh II (32)
1026	7.23	27.41	988	90.03	4.75			$\upsilon O_{31}{-}C_{32}$ (69)
1019	3.23	2.14	987	1.85	0.65			γCH I (89)
1017	34.75	4.43	976	0.25	0.82	976 m	974 m	γCH III (84)
1011	40.46	4.55	972	32.69	29.02	968 w		δMe I (49), υC_2C_{38} (38)
1002	5.37	4.71	956	1.98	1.17			γCH II (83), τCCCC II (10)
964	94.15	27.24	937	0.85	8.41			γCH II (81), τCCCC II (12)
953	0.58	4.03	919	3.36	13.07			δCCC I (33), δCCC III (30), δC=O (31)
922	5.48	10.50	911	0.07	3.54	908 w	909 w	γCH I (83)
889	18.91	0.85	854	23.13	2.85	860 w	861 w	γCH III (63)
873	58.18	2.22	846	6.90	1.69	848 w		γCH III (68)
865	13.72	2.24	830	28.50	7.50			γCH II (76)
859	8.97	2.37	826	8.68	11.15		826 m	γCH III (17), τCCCCQ (18), τCCCC III (15), γC=O (22)

(*continued on next page*)

Table 1 (*continued*)

HF/6-31G*			B3LYP/6-31G*			IR υ (cm^{-1})	Raman υ (cm^{-1})	Assignments
υ (cm^{-1})	IR intensity	Raman activity	υ (cm^{-1})	IR intensity	Raman activity			
844	7.36	2.11	820	36.54	13.09	824 vs		γCH II (63), δCCC III (23)
825	22.07	2.35	815	15.81	18.77			γCH II (84)
817	49.13	16.68	803	11.28	3.22		805 w	γCH I (52), γC═O (24)
785	2.62	1.54	774	14.26	16.14	778 s	787 m	υPh II (4), δCCC II (2), υC_{28}—O_{31} (25)
773	6.99	18.82	750	4.89	2.41	756 w	750 w	τCCCC III (40), τCCCC I (37), γC_5C_{21} (20)
753	6.50	1.87	730	32.16	2.53	733 m		τCCCC II (26), γCH I (36),
γC═O (35)								
746	60.81	2.71	728	11.30	3.77	726 s	727 w	τCCCC II (54), $\gamma C_{28}O_{31}$ (28)
713	3.8376	2.74	712	1.56	3.58		699 w	τCCCC II (37), δC═O (26), δCCC I (25)
683	4.70	2.11	671	1.14	7.31			δCCC III (77)
667	2.29	6.07	665	2.34	6.49	658 w		τCCCC I (50), τCCCC III (21), γC═O (22)
653	10.97	6.79	651	7.87	5.66	647 m	651 m	δCCC I (91)
642	4.76	5.83	638	1.68	5.80		636 w	δCCC II (57), τCCCC III (24)
598	18.26	0.81	595	9.67	2.19	589 w	599 w	δCCC Q (50), δCCC III (28)
596	21.02	1.06	581	12.29	2.36	574 s	580 w	γCC_{38} (28), γCC_{21} (27), τCCCC III (31)
559	17.10	1.57	548	15.93	0.96	546 s	545 w	τCCCC II (22), δCCC II (22), γCO_{31} (24), $\delta C_{28}O_{31}C_{32}$ (27)
539	17.64	3.76	537	15.07	11.85	527 w		γCO_{31} (26), τCCCC II (25), γCC_5 (28)
521	0.50	0.53	503	0.67	16.72			τCCCC I (35), τCCCC III (39), τCCCC Q (25)
478	1.53	19.93	480	1.37	27.56		487 s	γCCC Q (65), δCCC I (21)
465	0.58	0.83	466	0.43	0.28		465 w	δCCC Q (27), $\delta CC_{38}C$ (12), γCO_{31} (26), τCCCC II (15)
450	0.56	1.49	453	0.31	7.66			δCCO_{31} (38), $\delta C_{28}O_{31}C_{32}$ (27), δCCC Q (28)
438	1.96	0.41	429	1.25	1.11			τCCCC I (67), τCCCC Q (23)
432	1.50	2.48	425	1.02	3.40		423 w	τCCCC I (57), τCCCC III (29)
425	0.08	1.74	417	0.95	28.60			τCCCC II (76)
403	4.50	0.70	405	3.07	0.38			δCCC Q (27), $\delta CC_{38}C$ (25), τCCCC II (22)
393	29.93	0.93	392	28.40	0.19			δC═O (60), δCCC Q (26)
380	12.47	1.50	380	3.49	4.77			δCCC III (20), δC═O (25), τCCCC III (24)
365	0.67	4.78	364	0.79	7.29		364 w	γCC_{38} (32), τCCCC III (24), δCCC III (20)
323	1.41	6.10	321	1.47	4.37		329 m	δCCC Q (35), $\delta CC_{38}C$ (33), γCC_5 (32)
313	2.68	4.41	317	3.57	5.99			δCCC Q (57), δC═O (27)
259	3.19	3.57	262	2.42	1.97		261 w	$\delta C_{28}O_{31}C_{32}$ (51), δCCO_{31} (40)
243	0.99	4.12	246	1.86	8.55			τCCCC Q (59), γCC_{38} (32)
242	2.29	2.11	245	1.22	4.34			τMe II (46), τMe I (26)
235	1.35	0.29	238	0.89	0.92			τMe II (26), τMe I (64)
211	0.05	0.82	216	0.01	0.81		217 s	τMe II (53), γCC_5 (19)
200	0.80	6.35	200	0.81	8.53			δCCC III (22), δCCC II (22), τCCCC Q (29)
163	1.86	2.11	165	2.41	1.41		177 s	τCCCC Q (24), τCCCC II (21), $\tau CCO_{31}C_{32}$ (24)
158	3.37	0.24	159	1.62	2.13			τCCCC Q (39), τCCCC II (27), $\tau CCO_{31}C_{32}$ (21)
146	0.83	0.48	147	0.93	0.95		141 w	τCCCC Q (41), τCCCC III (34)
117	0.48	2.56	117	0.28	3.48		116 s	τCCCC Q (58), τCCCC I (28)
76	5.75	0.80	89	3.34	2.90		91 w	$\tau CCO_{31}C_{32}$ (61), τMe II (22)
74	0.43	1.68	79	0.31	10.37			τCCCC III (37), τCCCC Q (18), τMe I (20), $\tau CC_5C_{21}C$ (22)
45	1.62	5.35	54	0.91	11.45			$\tau CC_5C_{21}C$ (30), τCCCC Q (16), τCCCC II (14),τCCCC III (12)
31	3.36	2.64	33	2.41	4.33			τCCCC Q (47), τCCCC III (19), τMe I (20)
28	1.84	3.29	30	1.37	7.48			τCCCC Q (41), $\tau CC_5C_{21}C$ (12), τMe I (12)
20	2.78	6.61	22	2.62	5.33			τCCCC Q (53), $\tau CC_5C_{21}C$ (31)

υ-stretching; δ-in-plane deformation; γ-out-of-plane deformation; τ-torsional deformation; s-strong; v-very; m-medium; sh-shoulder; w-weak.

gave a γCH at 815 cm^{-1} and no band was experimentally observed for this mode. The in-plane and out-of-plane CH deformations, δCH and γCH of the phenyl ring are expected above and below 1000 cm^{-1}, respectively [30]. Generally, the CH out-of-plane deformations with highest wavenumbers have a weaker intensity than those absorbing at lower wavenumbers.

*4.2. Geometrical parameters and first hyperpolarizability of title compound **1***

No X-ray crystallographic data of this molecule has yet been established. However, the theoretical results obtained for **1** (Fig. 5) are almost comparable with the reported structural parameters of the parent molecule. From an X-ray crystal structure of anthraquinone itself, Murthy [38] reported the C═O bond length of the molecule in the crystal to be 1.224 Å. From X-ray crystal structures of substituted anthraquinones, it is evident that the C═O bond length depends on the substitution pattern. Thus, for 1,4-diphenylanthraquinone 1.223 Å [39], for a 1,8-bis(nicotinyl)anthraquinone, 1.212 Å and 1.205 Å, for a (1,8-bis(thiazolyl)anthraquinone lead complex 1.229 and 1.220 Å are given for the C═O bond lengths [40]. The authors' calculation of 1.25–1.26 Å for the C═O bond length of the title compound are reasonable in face of the above data. B3LYP/6-31G* calculations by Krishnakumar and Xavier [28] seem to give exaggerated bond lengths of 1.42 Å and 1.43 Å for the C═O groups in 1,5-dichloroanthraquinone.

Further calculated bond length values of title compound **1** (see Table S1), C_8—C_9 = 1.4829, C_9—C_{10} = 1.4048, C_9—C_{14} = 1.4037, C_{13}—C_{14} = 1.3950, C_{12}—C_{13} = 1.4042 Å are comparable to values, 1.478, 1.372, 1.395, 1.376, 1.410 Å obtained from the X-ray crystal structure of anthraquinone itself [38].

According to our calculations, at C_8 of **1**, the exocyclic angle C_9—C_8—O_{20} is reduced by 0.8° and C_4—C_8—O_{20} is increased by 2° from 120°, which shows the interaction between H_{37} and O_{20}. At C_7, there is also an interaction between H_{36} and O_{19}. This departure of the exocyclic angles from 120° can be found in the crystal structures of the anthraquinones, also [38]. In the energy minimized structure of **1**, the bond angle C_{24}—C_{28}—O_{31} is reduced by 4.5°

and C_{26}—C_{28}—O_{31} is increased by 4.5°, which shows the interaction between the methoxy group and H_{29}. It must be noted, however, that at room temperature in solution the methoxy group of **1** will freely rotate.

The anthraquinone core **1** is not planar as is evident from the calculated torsion angles, C_{13}—C_{14}—C_9—C_8 = −179.7, C_{14}—C_9—C_8—O_{20} = 8.1, C_{11}—C_{10}—C_9—C_8 = 179.4, C_{10}—C_9—C_8—O_{20} = −171.6, C_{12}—C_{11}—C_{10}—C_7 = 179.1, C_{11}—C_{10}—C_7—O_{19} = −1.9, C_{14}—C_9—C_{10}—C_7 = −178.6, C_9—C_{10}—C_7—O_{19} = 177.0, C_6—C_5—C_4—C_8 = 171.8, C_5—C_4—C_8—C_9 = 172.0, C_1—C_2—C_3—C_7 = 178.4 and C_2—C_3—C_7—C_{10} = 180.0°. Again, often the X-ray crystal structure of anthraquinones, especially of hindered arylanthraquinones, show a significant distortion of the anthraquinone core [41]. The torsion angles associated with the 4-methoxyphenyl substituent at C_5 of the anthraquinone core of **1** (denoted as PhII), as given by DFT calculations at its energy minimum, shows the substituent turned away from the median plane of the anthraquinone core, with torsion angles C_4—C_5—C_{21}—C_{22} = −62.2, C_4—C_5—C_{21}—C_{23} = 123.6, C_6—C_5—C_{21}—C_{22} = 115.4, C_4—C_5—C_{21}—C_{23} = 3.9°.

The first hyperpolarizability (β_0) of this novel molecular system was calculated using the B3LYP/6-31G*) method, based on the finite field approach. In the presence of an applied electric field, the energy of a system is a function of the electric field. The first hyperpolarizability is a third rank tensor that can be described by a $3 \times 3 \times 3$ matrix. The 27 components of the 3D matrix can be reduced to 10 components due to the Kleinman symmetry [42]. The components of β are defined as the coefficients in the Taylor series expansion of the energy in the external electric field. When the electric field is weak and homogeneous, this expansion becomes

$$E = E_0 - \sum_i \mu_i F^i - \frac{1}{2}\sum_{ij} \alpha_{ij} F^i F^j - \frac{1}{6}\sum_{ijk} \beta_{ijk} F^i F^j F^k - \frac{1}{24} \times \sum_{ijkl} \gamma_{ijkl} F^i F^j F^k F^l + \ldots$$

where E_0 is the energy of the unperturbed molecule, F^i is the field at the origin, μ_i, α_{ij}, β_{ijk} and γ_{ijkl} are the components of dipole moment, polarizability, the first hyperpolarizabilities, and second hyperpolarizabilities, respectively. The calculated first hyperpolarizability of the title compound is 17.9×10^{-30} esu, which is 137.69 times that of urea (0.13×10^{-30} esu) [43]. From this, we can deduce that the title compound and the series of compounds it represents are attractive candidates for further studies in non linear optical applications.

In order to investigate the performance and vibrational frequencies of the title compound, root mean square value (RMS) error between calculated and observed frequencies were evaluated using the following expression [44].

$\mathrm{RMS} = \sqrt{\frac{1}{n-1}\sum_i^n (\upsilon_i^{calc} - \upsilon_i^{exp})^2}$. The RMS error of the observed Raman bands and IR bands are found to be 27.83 and 38.82 for HF method and 10.32 and 12.45 for DFT method. The small differences between experimental and calculated vibrational modes are observed. The experimental results reported here are for the solid phase and theoretical calculations assume gaseous phase.

5. Conclusion

In conclusion, a vibrational analysis of the Raman and IR spectra of 1-(4-methoxyphenyl)-4-methylanthraquinone was carried out aided by DFT calculations of the molecule. The geometry is in general agreement with X-ray data that has been published for anthraquinone itself and for diaryl- and dihetaryl substituted anthraquinones. A computation of the first hyperpolarizability of the compound indicates that this class of substituted anthraquinones may be a good candidate as a NLO material.

Appendix A. Supplementary material

Supplementary data associated with this article can be found, in the online version, at doi:10.1016/j.molstruc.2011.07.060.

References

[1] J.M. Josien, N. Fuson, Bull. Soc. Chim. Fr. (1952) 389.
[2] J.E. Gautrot, P. Hodge, D. Cupertino, M. Helliwell, New J. Chem. 30 (2006) 1801.
[3] N.A. Shcheglova, D.N. Shigorin, N.S. Dokunikhin, Zh. Fiz. Khim. 40 (1966) 1048; N.A. Shcheglova, D.N. Shigorin, N.S. Dokunikhin, Chem. Abstr. 65 (1966) 9958b.
[4] N.A. Shcheglova, D.N. Shigorin, N.S. Dokunikhin, Zh. Fiz. Khim. 39 (1965) 3039; A. Shcheglova, D.N. Shigorin, N.S. Dokunikhin, Chem. Abstr. 64 (1965) 12058f.
[5] H.D.H. Showalter, E.M. Berman, J.L. Johnson, W.E. Hunter, Tetrahedron Lett. 26 (1985) 157.
[6] D.A. Orser (General Electric Company, Schenectady, NY, USA), US Pat. 3764549, October 9, 1973; D.A. Orser, Chem. Abstr. 79 (1973) 141431j.
[7] A. Matsuura, H. Sato, W. Sotoyama, A. Takahashi, M. Sakurai, J. Mol. Struct. THEOCHEM 860 (2008) 119.
[8] V. Sasirekha, V. Ramakrishnan, Spectrochim. Acta 70A (2008) 626.
[9] N. Yildiz, O. Polat, S.E. San, N. Kaya, J. Mol. Struct. 991 (2011) 127.
[10] S. Bi, D. Song, Y. Kan, D. Xu, Y. Tian, X. Zhou, H. Zhang, Spectrochim. Acta 62A (2005) 203.
[11] D. Jacquemin, V. Wathelet, J. Preat, E.A. Perpete, Spectrochim. Acta 67A (2007) 334.
[12] B. Wannalerse, T. Tuntulani, B. Tomaparanaget, Tetrahedron 64 (2008) 10619.
[13] R.M.F. Batista, S.P.G. Costa, M. Belsley, M.M.M. Raposo, Mater. Sci. Forum 636/637 (2010) 387.
[14] A. Krishnan, S.K. Pal, P. Nandakumar, A.G. Samuelson, P.K. Das, Chem. Phys. 265 (2001) 313.
[15] Y.R. Shen, The Principles of Nonlinear Optics, Wiley, New York, 1984.
[16] P.V. Kolinsky, Opt. Eng. 31 (1992) 1676.
[17] D.F. Eaton, Science 253 (1991) 281.
[18] C.R. Moylan, R.J. Twieg, V.Y. Lee, S.A. Swanson, K.M. Betterton, R.D. Miller, J. Am. Chem. Soc. 115 (1993) 12599.
[19] S. Gilmour, R.A. Montgomery, S.R. Marder, L.T. Cheng, A.K.Y. Jen, Y. Cai, J.W. Perry, L.R. Dalton, Chem. Mater. 6 (1994) 1603.
[20] T. Thiemann, Y. Tanaka, J. Iniesta, H.T. Varghese, C.Y. Panicker, J. Chem. Res. (2009) 732.
[21] M.J. Frisch, G.W. Trucks, H.B. Schlegel, G.E. Scuseria, M.A. Robb, J.R. Cheeseman, J.A. Montgomery, Jr., T. Vreven, K.N. Kudin, J.C. Burant, J.M. Millam, S.S. Iyengar, J. Tomasi, V. Barone, B. Mennucci, M. Cossi, G. Scalmani, N. Rega, G.A. Petersson, H. Nakatsuji, M. Hada, M. Ehara, K. Toyota, R. Fukuda, J. Hasegawa, M. Ishida, T. Nakajima, Y. Honda, O. Kitao, H. Nakai, M. Klene, X. Li, J.E. Knox, H.P. Hratchian, J.B. Cross, C. Adamo, J. Jaramillo, R. Gomperts, R.E. Stratmann, O. Yazyev, A.J. Austin, R. Cammi, C. Pomelli, J.W. Ochterski, P.Y. Ayala, K. Morokuma, G.A. Voth, P. Salvador, J.J. Dannenberg, V.G. Zakrzewski, S. Dapprich, A.D. Daniels, M.C. Strain, O. Farkas, D.K. Malick, A.D. Rabuck, K. Raghavachari, J.B. Foresman, J.V. Ortiz, Q. Cui, A.G. Baboul, S. Clifford, J. Cioslowski, B.B. Stefanov, G. Liu, A. Liashenko, P. Piskorz, I. Komaromi, R.L. Martin, D.J. Fox, T. Keith, M.A. Al-Laham, C.Y. Peng, A. Nanayakkara, M. Challacombe, P.M.W. Gill, B. Johnson, W. Chen, M.W. Wong, C. Gonzalez, J.A. Pople, Gaussian 03, Revision C.02 Gaussian, Inc., Wallingford CT, 2004.
[22] H.B. Schlegel, J. Comput. Chem. 3 (1982) 214.
[23] J.B. Foresman, in: E. Frisch (Ed.), Exploring Chemistry with Electronic Structure Methods: A Guide to Using Gaussian, Gaussian, Pittsburg, PA, 1996.
[24] J.M.L. Martin, C. Van Alsenoy, GAR2PED: A Program to Obtain a Potential Energy Distribution from a Guassian Archive Record, University of Antwerp, Belgium, 2007.
[25] Spectral Database for Organic Compounds SBDS, Institute of Advanced Industrial Science and Technology.
[26] S.E. Jorge-Villar, H.G.M. Edwards, J. Raman Spectrosc. 41 (2010) 63.
[27] A. Baran, B. Wrzosek, J. Bukowska, L.M. Proniewicz, M. Branska, J. Raman Spectrosc. 40 (2009) 436.
[28] V. Krishnakumar, R.J. Xavier, Spectrochim. Acta 61 (2005) 1799.
[29] N.B. Colthup, L.H. Daly, S.E. Wiberly, Introduction to Infrared and Raman Spectroscopy, third ed., Academic Press, Boston, 1990.
[30] N.G.P. Roeges, A Guide to the Complete Interpretation of the Infrared Spectra of Organic Structures, Wiley, NewYork, 1994.
[31] G. Socrates, Infrared Characteristic Group Frequencies, Wiley, Interscience Publication, New York, 1980.
[32] P. Sett, N. Paul, S. Chattopadhyay, P.K. Mallick, J. Raman Spectrosc. 30 (1999) 277.
[33] P. Sett, S. Chattopadhyay, P.K. Mallick, Spectrochim. Acta 56A (2000) 855.
[34] P. Sett, S. Chattopadhyay, P.K. Mallick, J. Raman Spectrosc. 31 (2000) 177.
[35] J.H.S. Greeb, Spectrochim. Acta 24 (1968) 1627.
[36] G. Varsanyi, Assignments for Vibrational Spectra of Seven Hundred Benzene Derivatives, Wiley, New York, 1974.
[37] K.R. Ambujakshan, V.S. Madhavan, H.T. Varghese, C.Y. Panicker, O. Temiz-Arpaci, B. Tekiner-Gulbas, I. Yildiz, Spectrochim. Acta A 69 (2008) 782.

[38] B.V.R. Murthy, Z. Kristallogr. 113 (1960) 445.
[39] J.E. Gautrot, P. Hodge, D. Cupertino, M. Helliwell, New. J. Chem. 31 (2007) 1585.
[40] M. Kadarkaraisamy, D. Mukherjee, C.C. Soh, A.G. Sykes, Polyhedron 26 (2007) 4085.
[41] L. Lunazzi, M. Mancinelli, A. Mazzanti, J. Org. Chem. 74 (2009) 1345.
[42] D.A. Kleinman, Phys. Rev. 126 (1962) 1977.
[43] M. Adant, I. Dupuis, L. Bredas, Int. J. Quantum. Chem. 56 (2004) 497.
[44] L. Ushakumari, H.T. Varghse, C.Y. Panicker, T. Ertan, I. Yildiz, J. Raman Spectrosc. 39 (2008) 1832.